

# Crystal structure of a charge-control agent of the quaternary ammonium salt and its electrical properties

Kazuya Uta, Yohei Sato, and Jin Mizuguchi; Graduate School of Engineering, Yokohama National University; 79-5 Tokiwadai, Hodogaya-ku, 240-8501 Yokohama, Japan

## Abstract

The title compound (P-51) is a well-known charge-control agent (CCA) used widely in electrophotography. Structure analysis as well as electrical measurements has been carried out in the present study in order to support our charge-control mechanism that assumes an appreciable temperature increase at the “toner/carrier” interface. P-51 is found to crystallize in space group of  $P2_1/n$ . There are chains of  $\text{OH}\cdots\text{O}$  intermolecular hydrogen bonds between the OH group of one anion and the O atom of the other, leading to a polymer-like stabilization of the anion. The electrical conductivity increases exponentially with temperature by two-three orders of magnitude in the temperature range between room temperature and 100 °C. The present temperature dependence is closely correlated with the molecular arrangement as well as charging characteristics of the toner which includes P-51.

## 1. Introduction

The title compound (quaternary-ammonium salt, P-51; Fig. 1) is a charge-control agent (CCA) of the positive type used in electrophotography that creates a desired charge level and polarity. A number of investigation have been carried out on the charge-control mechanism on the basis of the work function,<sup>1)</sup> mass transfer<sup>2)</sup> and charge transfer.<sup>3)</sup> However, no clear-cut, consistent explanation has been established yet at the moment. In view of the present situation, we have recently proposed a novel model that assumes an appreciable temperature increase at the “toner/carrier” interface due to the tribo-electrification.<sup>4)</sup> Because of the present local and instantaneous heating, the electrical conductivity of CCA (which resides on the surface of both toner and carrier) is remarkably increased to give a conductive channel, through which the carrier-flow occurs effectively to charge up the toner. These two assumptions have experimentally been verified.<sup>4)</sup> Especially, the local heating up to around 100 °C has been confirmed by using a pigment-marker (ethylp yridyl perylene-imide) which changes its color from black (*trans* form) to red (*cis* form). Around this temperature, the electrical conductivity of CCA increases appreciably by two-three orders of magnitude as compared with that of room temperature.

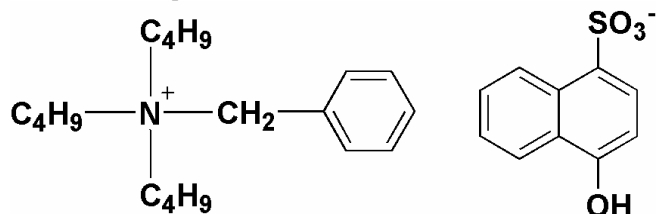


Fig. 1 Molecular structure of P-51.

The purpose of the present investigation is to clarify the crystal structure of P-51 as well as to study the correlation between the crystal structure, temperature dependence of the electrical conductivity and the charging characteristic of the toner which includes P-51.

## 2. Experiment

### 2.1 Materials and crystal growth of P-51

P-51 (melting point: ca 190 °C) is a commercial product of Orient Chemical Industries Ltd. Single crystals were grown by recrystallization from a methanol solution. After 48 h, a number of colorless crystals were obtained in the form of blocks (Fig. 2: 0.49×0.26×0.17 mm<sup>3</sup>).

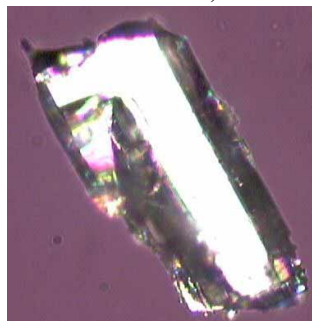


Fig. 2 Single crystal of P-51.

### 2.2 Data collection and X-ray structure analysis

Reflection data were collected on a R-Axis RAPID-F diffractometer from Rigaku using  $\text{CuK}\alpha$  radiation ( $\lambda = 1.5418 \text{ \AA}$ ) at room temperature and -180 °C. The structures were solved by direct methods (SIR2004<sup>5)</sup>) and refinement was carried out by the full-matrix least-squares method on  $F^2$  (SHELXS-97<sup>6)</sup>).

### 2.3 Preparation of samples for electrical measurements

Measurements of the electrical conductivity in the form of powders are generally not reproducible and reliable due to the packing density of the powder as well as the electroding problems. Therefore, two kinds of samples were prepared: recrystallized sample from a methanol solution and fused sample prepared by heating above the melting point, followed by gradual cooling. The former was directly prepared on ITO (Indium-Tin-Oxide) interdigital electrodes by spin coating (Fig.3(a)); whereas the latter was made in a capillary of 2.3 mm in diameter, using the Cu-rods as the electrodes (Fig. 3(b)).

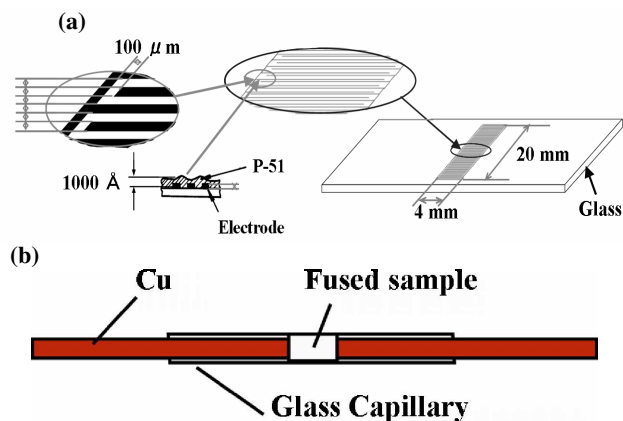


Fig. 3: (a) Recrystallized sample. and (b) fused sample.

## 2.4 Measurements

The temperature dependence of the electrical conductivity was measured on the above two samples, with a 6514 Keithley electrometer, in the temperature range between room temperature and 200 °C at a heating rate of 3 K/min.

Thermogravimetric analysis (TGA) and differential thermal analysis (DTA) were made in air on commercial powders, recrystallized powders and fused powders of P-51 at a heating rate of 10 K/min, using a Rigaku Thermo Plus TG-8120.

The temperature dependence of powdered X-ray diffraction was measured with a RAPID-F on commercial powders as well as on fused powders of P-51 in the temperature range between room temperature and 200 °C.

Tribo-electrification measurements were made on toners composed of styrene acryl resin (100 parts), carbon black (6 parts), wax (2 parts) and CCA (1 part) in accordance with the standard procedure specified by ISJ, using a blow-off equipment (TB-200: Toshiba Chemical).

## 3. Results and discussion

### 3.1 Crystallographic parameters for P-51

Table. 1 Crystallographic parameters for P-51.

	High temp. phase (23 °C)	Low temp. phase (-180 °C)
Formula	$C_{29}H_{41}NO_4S$	
Molecular weight	499.71	
Crystal system	monoclinic	
Molecular symmetry	$C_1$	$C_1$
Space group	$P2_1/n$	$C2/c$
$a$ (Å)	14.381	28.127
$b$ (Å)	9.812	19.638
$c$ (Å)	19.776	24.260
$\beta$ (°)	92.560	126.851
Density (g/cm <sup>3</sup> )	1.190	1.393
$Z$	4	18

Table 1 details the crystallographic parameters for P-51 measured at room temperature and -180 °C, showing two different phases of the monoclinic system. Among these, only the room-temperature structure ( $P2_1/n$ ) has been successfully solved.

Fig. 4 shows the ORTEP plot of P-51. The molecule has no center of symmetry (*i.e.*  $C_1$ ), but a pair of the molecules reside on an inversion center. Since one negative charge is delocalized in the form of  $SO_3^-$ , no significant difference in S-O bond length is recognized between these three bonds.

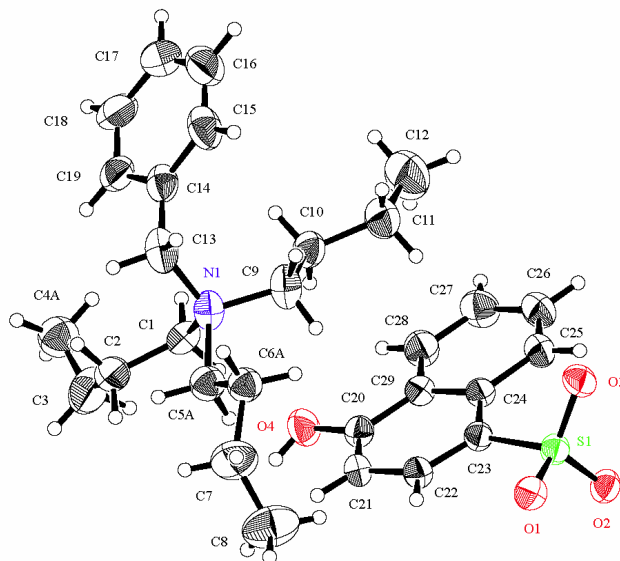


Fig. 4 ORTEP plot of P-51.

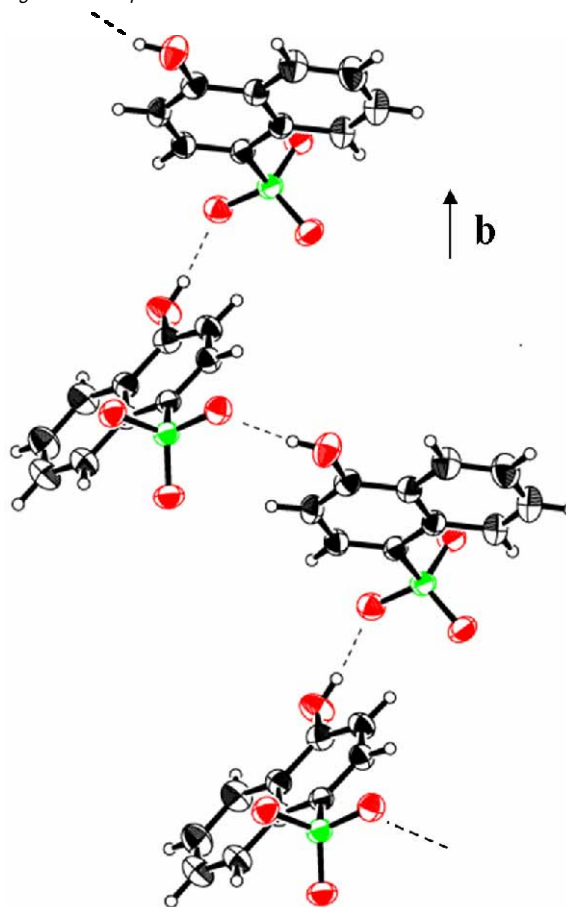


Fig. 5 Hydrogen-bond network along the  $b$ -axis.

It is important to note that there are chains of OH...O intermolecular hydrogen bonds along the *b*-axis between the OH group of one anion and the O atom of another as shown in Fig. 5. The present hydrogen bonds impart a polymer-like stabilization to the anion network, raising the melting point higher.

### 3.2 Powder X-ray diffraction diagrams

Fig. 6 shows the powder X-ray diffraction diagrams for commercial powder of P-51, recrystallized powder and fused powder.

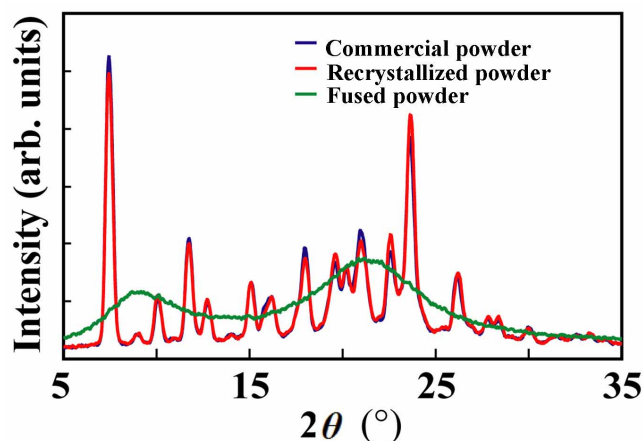


Fig. 6 Powder X-ray diffraction diagrams for P-51.

The diagram of the commercial powder coincides perfectly with that of the recrystallized one. However, the fused powder exhibit entirely different diffraction diagrams as characterized by amorphous-like poor crystallinity.

### 3.3 Temperature dependence of the electrical conductivity

Fig. 7 shows the temperature dependence of the electrical conductivity (*i.e.* Arrhenius plot) for recrystallized P-51 and fused samples together with styrene-acryl (St-Ac) polymer used commonly in toners.

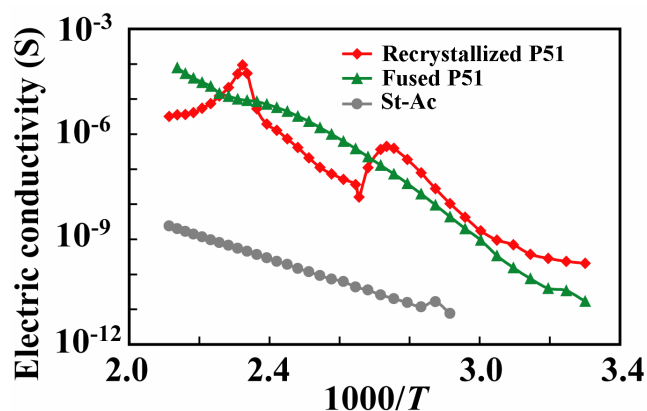


Fig.7 Temperature dependence of the electrical conductivity for various P-51 samples.

The electrical conductivity increases linearly with temperature in these samples, showing semiconductor-like behavior. The electrical conductivity of St-Ac polymer is lower than that of P-51 samples by two-three orders of magnitude.

It is remarkable to note that recrystallized P-51 exhibits two bumps, peaking at about 93 and 157 °C. On the other hand, P-51 shows no bumps, but is characterized by a swell in the whole temperature range. In both samples, the electrical conductivity at 100 °C is higher by two-three orders of magnitude as compared with that of room temperature. This bears out our charge-control model described in Introduction.

### 3.4 TGA/DTA curves

Fig. 8 shows the TGA/DTA curves for P-51 powders as supplied, or recrystallized, or fused.

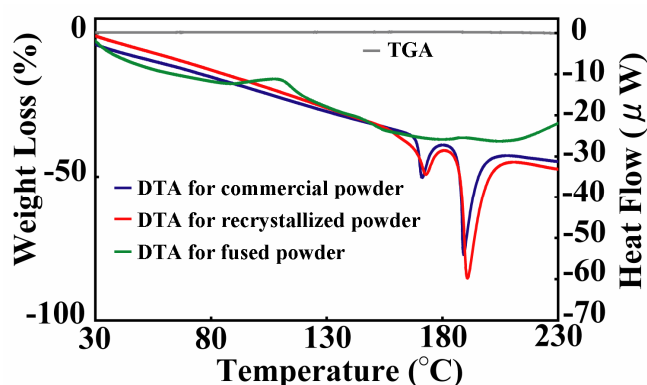


Fig. 8 TGA/DTA for various P-51 samples.

No weight-loss is observed in those samples, but their DTA curves are drastically different. P-51 as supplied or recrystallized exhibits an endothermic gradual curve, ending up with two peaks around 171 and 189 °C. The second peak around 189 °C corresponds to the melting point of P-51. On the other hand, the first peak around 171 °C corresponds to the bump in the electrical conductivity (Fig. 7). This indicates that a small change in molecular arrangement might have occurred at this temperature. However, no endothermic peak is observed in the DTA curve which corresponds to the bump around 96 °C in the electrical conductivity.

On the other hand, P-51 as fused show a very broad, endothermic curve which includes the small, broad maxima around 88, 179 and 207 °C. In the temperature dependence of the electrical conductivity, no bump but a very broad swell is recognized as shown in Fig. 7.

### 3.5 Temperature dependence of the powder X-ray diffraction diagrams

Fig. 9 shows the diffraction diagrams for P-51 as recrystallized at 20, 120 and 160 °C. The phase at 20 °C is identified as the same phase as the single crystal.

No noticeable difference is observed in diffraction diagrams up to 120 °C. Then, one can see some changes in diffraction peaks around  $2\theta = 7, 13, 21$  and  $23.5^\circ$ . This is indicative of the change

in molecular arrangement and corresponds to the bump in electrical conductivity around 157 °C (Fig. 7).

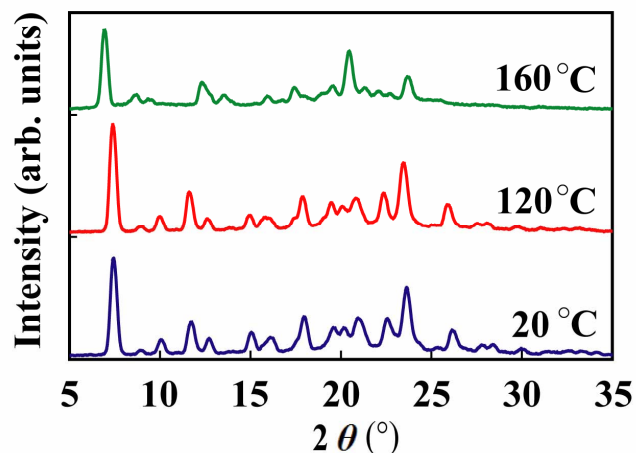


Fig. 9 Diffraction diagrams of commercial P-51 at 20, 100 and 160 °C.

### 3.6 Tribo-electrorification of toners which includes variously-treated P-51s

Fig. 10 shows the charging characteristics as a function of time.

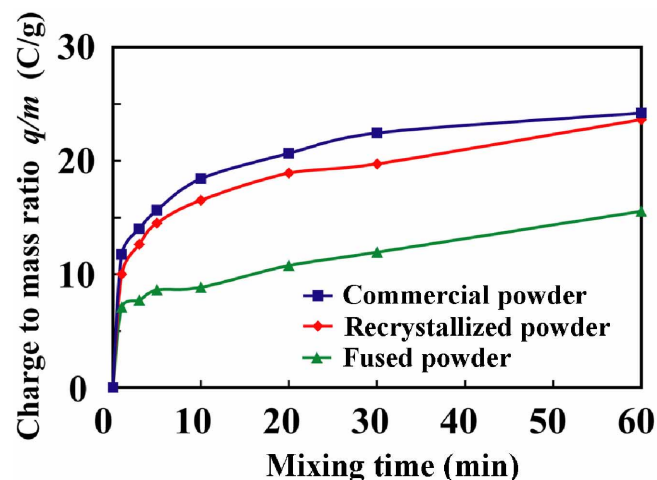


Fig. 10 Charging characteristics for various toners which include P-51.

P-51 as supplied or as recrystallized exhibits an excellent characteristic; whereas the amount of charge of the fused P-51 is much lower than that of the former two samples, although no difference in charging rate is recognized in these three samples.

Figs. 11(a), 11(b) and 11(c) are the SEM pictures for P-51 as supplied, as recrystallized and as fused, respectively. These are the sieved samples through meshes of 5  $\mu\text{m}$ . A number of crystallites characterized by beautiful habits are observed in commercial P-51 and P-51 as recrystallized. On the other hand, powdered P-51 as fused lacks this property and appears brittle. This is presumably indicative of an amorphous-like state.

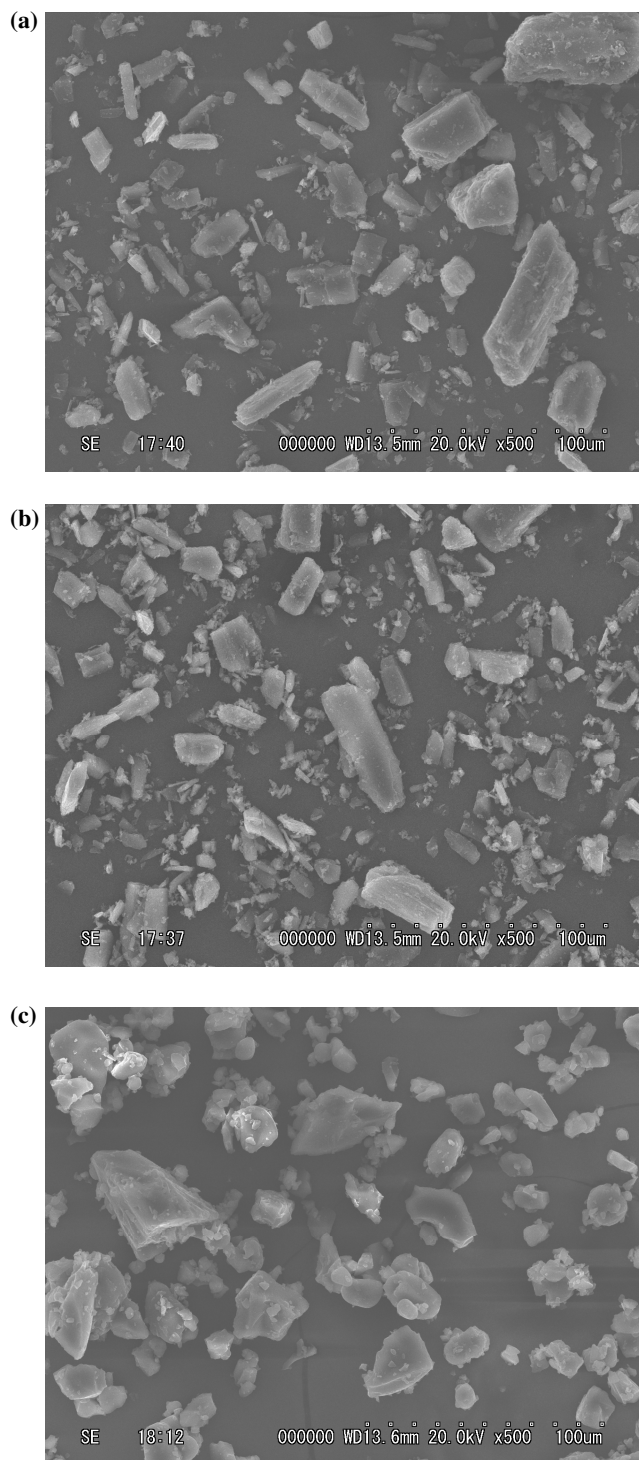


Fig. 11 SEM pictures: (a) Commercial P-51, (b) P-51 as recrystallized and (c) P-51 as fused.

#### 4. Conclusions

The conclusions drawn from the present investigation can be summarized as follows

1. P-51 is found to crystallize in space group of  $P2_1/n$  at room temperature. However, there found also another phase at  $-180^\circ\text{C}$  ( $C2/c$ ). There are chains of  $\text{OH}\cdots\text{O}$  intermolecular hydrogen bonds in anions which stabilize the anion system.
2. The phase of commercial P-51 coincides with that of P-51 as recrystallized. However, the phase as fused is different and characterized by amorphous-like, poor crystallinity.
3. The temperature dependence of the electrical conductivity of P-51s as recrystallized or as fused shows an increase in electrical conductivity by two-three orders of magnitude with increasing temperature. However, P-51 as recrystallized shows two bumps in electrical conductivity which is closely related to the change in molecular arrangement as shown by thermal analysis.
4. Commercial P-51 or P-51 as recrystallized exhibits an excellent charge-control characteristic; whereas P-51 as fused shows a lower saturation potential, although no noticeable difference is recognized in charging rate.

#### References

- [1] R.J. Nash, M.L. Grande and R.N. Muller, "CCA Effects on the Triboelectric Charging Properties of a Two-Component Xerographic Developer", Proceedings of IS & T's NIP 17, 358 (2001).
- [2] A. Suka, M. Takeuchi, K. Suganami and T. Oguchi, "Toner Charge Generated by CCA Particles at the Interface between Toner and Carrier", J. Imag. Soc. Jpn. 45, 127-132 (2006).
- [3] J. Guay, J. E. Ayala, and A. F. Diaz, "The Question of Solid-State Electron Transfer in Contact Charging between Metal and Organic Materials", Chem. Mater, 3, 1068-1073 (1991).
- [4] J. Mizuguchi, A. Hitachi, Y. Sato and K. Uta: Proceedings of ICJ2006 Fall Meeting, A study of the charge control mechanism, pp121-124.
- [5] M.C. Burla, M. Camalli, B. Carrozzini, G.L. Cascarano, C. Giacovazzo, G. Polodori & R. Spagna. (2003). J. Appl. Cryst. 36, 1103
- [6] G.M. Sheldrick, (1997). SHELXL97. University of Gottingen, Germany.

#### Author Biography

*Kazuya Uta received his Bachelor of Engineering from Yokohama National University in 2007. He is currently in the graduate course for applied physics at the same university. His research interest includes a charge-control mechanism of CCA (Charge Control Agent). He is a member of the Chemical Society of Japan and The Imaging Society of Japan. E-mail: d07gd203@ynu.ac.jp.*